



# Optical Benchmarking of a Novel Polar Bi-Focal Beam-Down Tower Concept

Peter Schöttl<sup>1</sup>, Gregor Bern<sup>1</sup>, and Francisco Torres<sup>1</sup>

<sup>1</sup> Fraunhofer Institute for Solar Energy Systems ISE, Germany

**Abstract.** Small-scale modular CSP systems using polar heliostat field arrangements reduce cosine losses significantly and – by integrating a secondary beam-down reflector – enable novel receiver concepts. A novel polar bi-focal beam-down design is introduced and its optical performance is assessed with ray tracing. Albeit not fully optimized, results show that – in comparison to a single-focus beam-down system – the bi-focal system entails higher annual, DNI-weighted optical efficiency and flatter circadian profiles, beneficial for reducing peak dumping. Even higher optical performances can be reached by combining single-focus and bi-focus systems.

**Keywords:** Central Receiver Solar Tower, Beam-Down, Bi-Focus

## 1. Introduction

In recent years, several CSP companies (e.g. Vast Solar, 24/7 Solar, Magaldi or HelioGen) have suggested small, modular Solar Tower systems, as opposed to large-scale systems with several 100 MW<sub>th</sub> (e.g. Noor-3, Cerro Dominador or Yumen Xinneng). This is economically viable, if

- many such modular units are coupled to a central powerblock – the specific costs of steam turbines decrease with their size [1],
- small, decentral power cycles are used, e.g. supercritical CO<sub>2</sub> or gas turbines,
- a single unit supplies an industrial or solar-fuel process with high-temperature heat.

By integrating a secondary beam-down reflector, the (heavy) receiver can be placed on the ground. This reduces both pumping losses and tower structure costs and makes alternative receiver concepts possible in the first place (e.g., fluidized bed with open top as implemented in the Magaldi STEM system). Particularly the latter aspect is not considered in a rather critical review of the beam-down technology by Vant-Hull [2], from which some arguments are discussed and rebutted herein. A recent review on beam-down systems is given by Bellos [3].

With smaller module sizes, the heliostat slant ranges (heliostat distance to the focal point) and consequently the atmospheric attenuation losses are smaller. This enables polar heliostat fields on one side of the receiver, which – as opposed to surround fields common for large-scale Solar Tower systems – exhibit strongly reduced cosine losses, particularly for locations with high latitudes [4].

Even for polar systems, the cosine losses still represent the largest optical loss. Therefore, we are suggesting a polar bi-focus beam-down (BFBD) system, where the heliostats switch their focus between two secondaries/receivers depending on the sun position. This allows for a further reduction of cosine losses as compared to single-focus Solar Towers (ST) or single-

focus beam-down (SFBD) systems. Focus-switching solar tower systems have been studied by Arbes et al. [5], resulting in a rather negative evaluation. However, they used a very different concept based on surrounding heliostat fields.

To ensure an overall high utilization ratio of the costly receivers, the BFBD needs to be realized as a multi-unit system (see Figure 1), where the receivers get concentrated radiation either from their west or east neighboring heliostat field. This means that each heliostat field unit has two affiliated secondary reflectors and receivers.

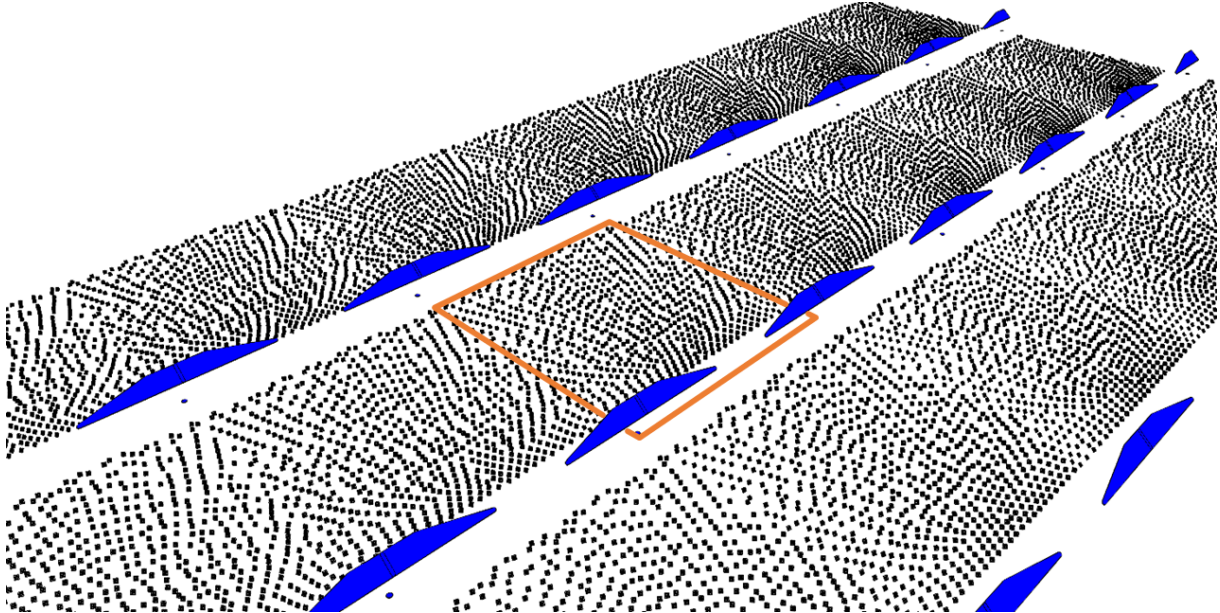


**Figure 1.** Multi-unit BFBD system. A single unit (heliostat field, two affiliated beam-down reflectors and receivers) is marked with an orange outline.

In this study, a BFBD system is designed alongside with a comparable SFBD and a comparable conventional ST. An adapted BFBD featuring both single- and bi-focus regions is added as a fourth configuration. For a reference site in Yumen, China, all configurations are assessed in terms of their annual optical performance and benchmarked against each other. Their circadian optical efficiency curves are compared. Eventually, the assessments are carried out for three additional typical CSP sites with different latitudes.

## 2. System design and performance evaluation methodology

### 2.1 Heliostat field design

Heliostat fields with a single focus point (ST, SFBD, parts of adapted BFBD) are herein designed using an enhanced MUEEN algorithm [6,7], which aims at avoiding blocking between heliostats. As the underlying radially staggered pattern only works for systems with a single target, a different approach has been applied for the bi-focus configurations. Based on a graphical tool that visualizes the blocking shadow projection for each heliostat and both aim points, heliostats were placed manually, such that the blocking shadow overlaps are as small as possible and – at the same time – the heliostats are close to the tower.

While yielding reasonable heliostat fields, the presented manual approach is tedious, and results are sub-optimal. Thus, BFBD performance results as presented in section 4 can be considered as a baseline of what is possible with such a system. Wrapping the approach in an automated algorithm is work in progress.

## 2.2 Secondary reflector design

For simplicity's sake, the secondary reflectors for both SFBD and BFBD systems were designed as flat polygons, in a five-step approach:

1. An anchor point for the secondary is selected at the defined tower height.
2. The secondary's surface normal is calculated such that a ray from a selected central heliostat in the field to the anchor point is reflected downwards to the center of the receiver. With anchor point and surface normal, the secondary plane is fully defined.
3. By extending the vector from the selected heliostat to the anchor point by the distance between anchor point and receiver center, the virtual aim point is determined.
4. The vectors from the pre-defined heliostat field corners to the virtual aim point are calculated. The intersection points of these vectors with the secondary plane provide the secondary corners points.
5. To account for the beam spread of the heliostats at the borders of the field, a rim area with rounded edges is added to the outline defined by the corner points calculated as described above in 4.

This approach guarantees that the secondary is large enough to avoid excessive spillage, yet it minimizes its shading effect on the heliostat field. With a flat secondary, the virtual aim point obtained from the above-described procedure is valid for all heliostats.

## 2.3 Annual, DNI-weighted assessment based on ray tracing

Optical losses and efficiency are evaluated with the Fraunhofer ISE in-house software suite Raytrace3D [8]. To obtain annual results, ray tracing simulations are carried out for the nodes of a sky discretization [9], then interpolated for the sunshine hours of the year and integrated with DNI weighting. DNI data is exported from Meeonorm [10] for the different sites.

## 3. System configurations

To achieve a certain level of comparability, several parameters are predefined and equal for all four configurations, roughly resembling the dimensions of the PS10 system in Spain [11] with a 50 MW<sub>th</sub> receiver. Most notably, this is the number and dimensions of the heliostats, the available field area, the tower height and the receiver size. Table 1 lists the main system parameters.

It should be noted that the selected parameters are not the result of a thorough optimization. Hence, performance evaluation results do not represent the achievable optimum. All four configurations are schematically depicted in Figure 2, designed for the north hemisphere.

In the ST configuration, the tower is integrated as an opaque cylinder (concrete) with a diameter of 13 m. The beam-down reflectors are held by steel lattice structures, whose shading effect is assumed to be negligible. On the contrary, the large secondary reflectors themselves have a considerable shading effect, visible in the simulation results.

For the ST and SFBD configurations, the ideal heliostat focal length is trivially equal to the slant range. In the BFBD configuration, the focal length is chosen equal to the distance to the farther aim point, which results in the lowest spillage. For the ST and SFBD configurations, the heliostats trivially aim at the receiver center and at the virtual aim point respectively. In the BFBD configuration, the heliostats switch between the two virtual aim points, based on minimizing the incidence angle on the heliostat with respect to the sun position.

**Table 1.** Configurations ST, SFBD, BFBD and adapted BFBD. Main system parameters.

	ST	SFBD	BFBD	adapted BFBD
Heliostat field design	MUEEN	MUEEN	Shadow projection	MUEEN + Shadow projection
Heliostat field outline	800 m x 800 m			
No. of heliostats	750			
Mirror area	10 m x 10 m			
Heliostat reflectance	93%			
Heliostat slope error	1 mrad			
Heliostat tracking mode	Azimuth-elevation			
Receiver shape	Disc-shaped aperture			
Receiver area	169 m <sup>2</sup>			
Receiver altitude	100 m	0 m	0 m	0 m
Receiver absorptance	100%			
Secondary shape	-	Flat polygon with rounded edges		
Secondary reflectance	-	93%		
Secondary slope error	-	1 mrad		
Secondary altitude	-	100 m		

The analysis of the BFBD system (see Section 4.2) showed that the east and west parts of the BFBD heliostat field benefit the least from the cosine loss reduction, while having comparatively high spillage. This finding led to the creation of an adapted BFBD design (BFBD\_adapt), where only the central part (within +/- 200 m in west-east-direction – an educated guess) switches between the focus points, while the west/east parts always aim at their closest focus point. This implies that the west/east parts of the heliostat field can be designed with the MUEEN algorithm and the respective heliostats' focal length is equal to the slant range. The determination of single-focus and bi-focus regions was not the result of a thorough optimization and leaves room for improvement. Figure 2 visualizes that the heliostats for the ST and SFBD configurations and the west/east part of the adapted BFBD follow the radially-staggered pattern of the enhanced MUEEN algorithm. For the BFBD system – where heliostats have been placed manually based on a blocking visualization tool, no uniform pattern is discernible, apart from exploiting the symmetry of the arrangement. Furthermore, the BFBD placement with two blocking constraints to be considered and created with the manual tool visibly requires more land area.

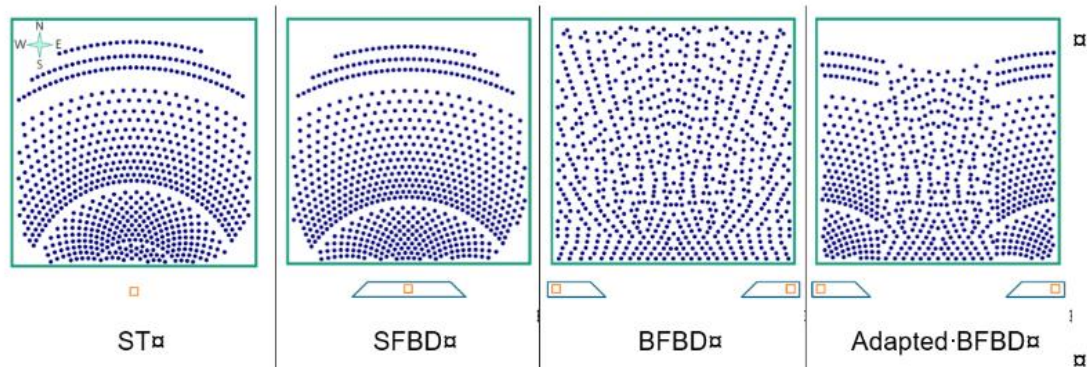


**Figure 2.** Configurations ST, SFBD, BFBD, adapted BFBD. Heliostat base points and schematic representation of heliostat field outlines (green frame), receivers (orange rectangles) and secondary beam-down reflectors (blue frames).

## 4. Optical benchmarking results and discussion

As a reference site for this study, Yumen, China (40.4N, 97.3E) has been selected, which has a comparatively high latitude. Section 4.4 expands on three other sites.

### 4.1 Annual, DNI-weighted optical losses and efficiency

All optical losses are represented as loss contributions with respect to the originally available radiation, not as fractions relative to the radiation available in the previous optical stage. Figure 3 shows a comparison of optical losses and efficiency for all four configurations.

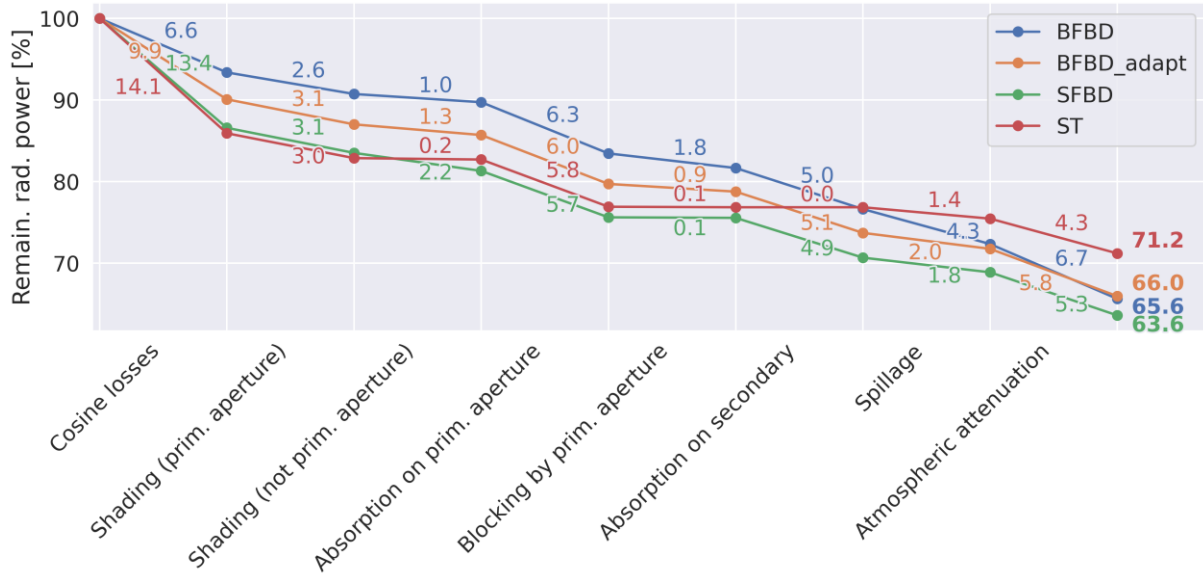


**Figure 3.** Configurations ST, SFBD, BFBD and adapted BFBD. Annual, DNI-weighted optical losses and efficiency as waterfall diagram.

Amongst the four compared systems, the ST configuration has the highest annual optical efficiency of 71.2%, as opposed to the SFBD configuration with 63.6%. This is primarily attributed to the lack of shading and absorption losses on the non-existent beam-down reflector. Furthermore, the radiation path lengths from heliostat to receiver are shorter, leading to reduced spillage and atmospheric attenuation.

The BFBD configuration exploiting the focus switching has cosine losses reduced by more than half compared to the single-focus systems. On the negative side, there is more blocking in the heliostat field (attributable to the sub-optimal, manual heliostat placement) and stronger spillage and atmospheric attenuation. The latter two are primarily caused by longer radiation path lengths. Relatively, the BFBD's annual optical efficiency is 3.1% higher than its SFBD counterpart.

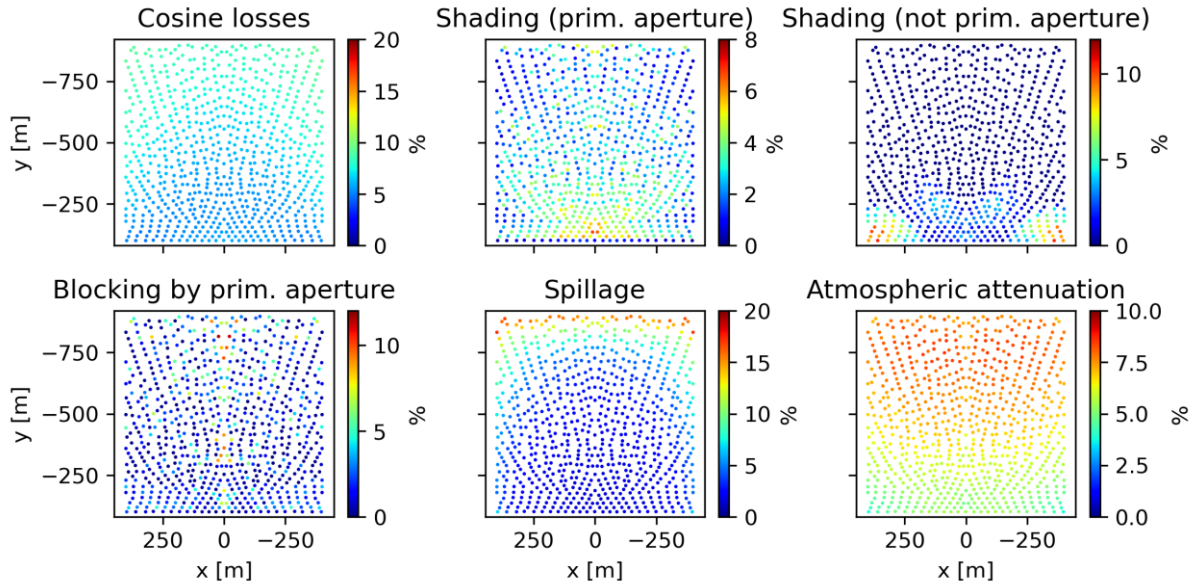
Compared to BFBD, the adapted BFBD configuration has higher cosine losses, yet lower blocking, spillage and atmospheric attenuation, giving it a small lead of 0.4%-pts in annual efficiency. The difference might be larger for an optimal selection of single-focus and bi-focus regions. As explained above, there is a lot of potential for optimization of the heliostat field layout.

### 4.2 Assessment of individual heliostats

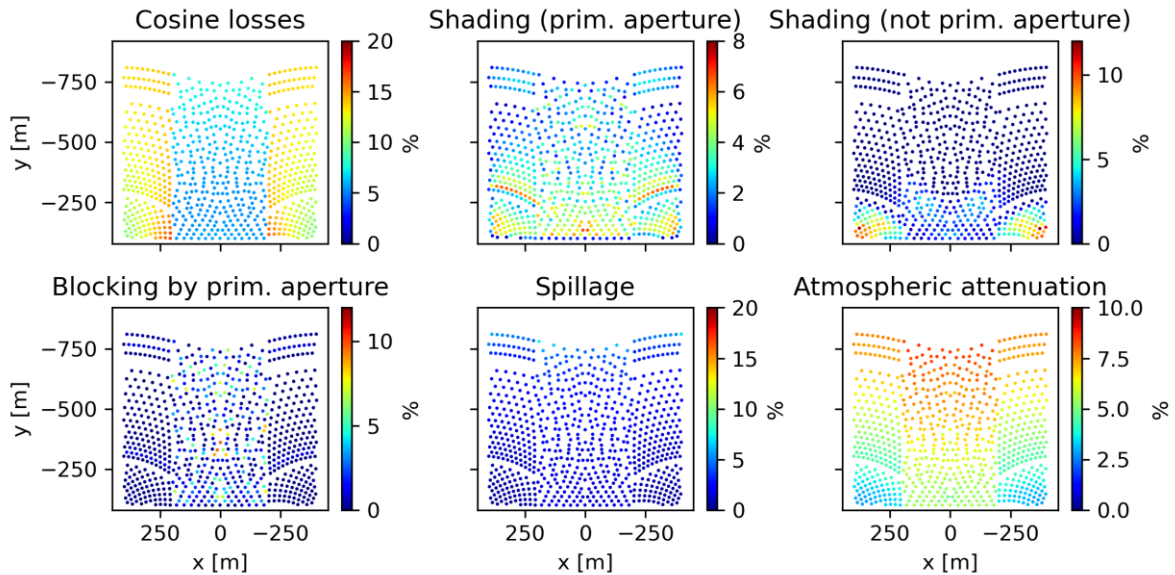
For deep analysis, the spatial distribution of relevant optical losses in the heliostat field is discussed. As a time- and angle-invariant reflectance is assumed for the primary and secondary mirrors, absorption losses on heliostats and secondary reflectors are excluded. Figure 4 and



Figure 5 show the cosine losses, the shading due to other heliostats (prim. aperture) and due other structural elements (not prim. aperture), blocking, spillage and atmospheric attenuation, for the BFBD and adapted BFBD configurations respectively. The comparison between these two configurations has been selected, as it explains both single-focus and bi-focus modes of operation and illustrates the thought process behind the design of the adapted BFBD. The color maps are consistently scaled to allow for comparisons between the two figures.



**Figure 4.** Configuration BFBD. Loss contributions for individual heliostats based on annual, DNI-weighted assessment.



**Figure 5.** Configuration adapted BFBD. Loss contributions for individual heliostats based on annual, DNI-weighted assessment.

As expected, cosine losses for BFBD are consistently low, while they are increased in the single-focus west/east region of the adapted BFBD configuration. Relevant shading by other heliostats can be observed for both configurations particularly in the regions closer to the aim points, as both heliostat field designs – aiming for reduced blocking – allow denser heliostat placement there. Shading due to other elements is naturally visible in the south-west and south-east region, due to the shadow of the beam-down reflectors. The imperfect manual he-

liostat placement leads to increased blocking in the entire BFBD configuration and in the central part of the adapted BFBD. The latter's west/east regions designed with the enhanced MUEEN algorithm exhibit almost zero blocking. Spillage is primarily noticeable in the northern sections of the BFBD configuration. This is because the respective heliostats are positioned farther from the secondary reflectors and receivers, and their slant ranges additionally increase when they are oriented towards the aim point that is further away. For both configurations, atmospheric shows a spatial trend comparable to spillage, yet with smoother transitions.

### 4.3 Seasonal profiles

Figure 6 shows the circadian profiles of optical efficiency at summer/winter solstice and at the equinox, for both the SFBD and the BFBD configuration.

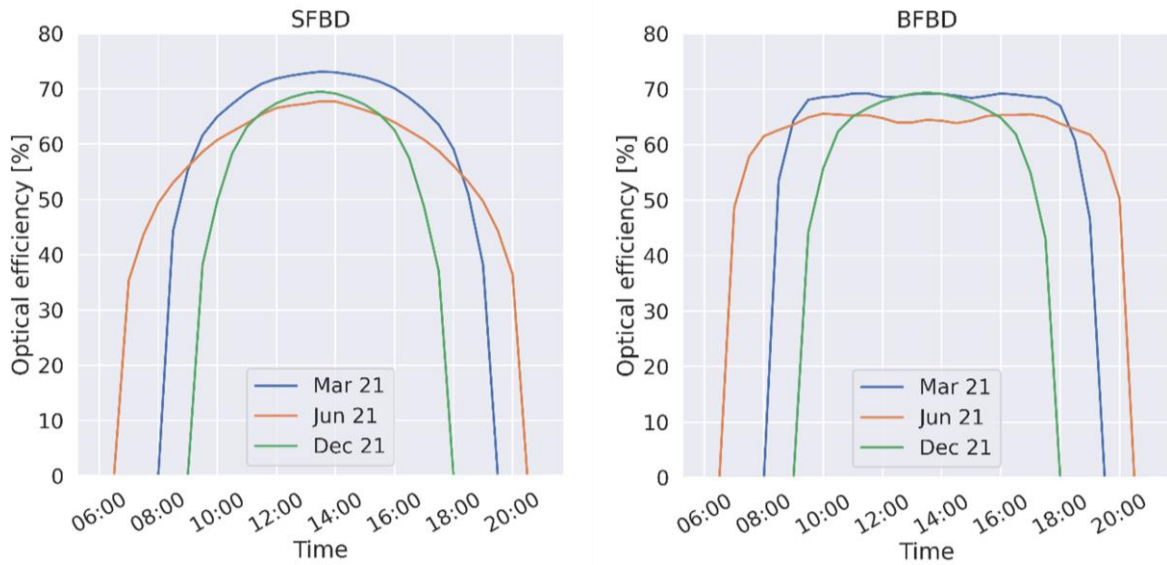


**Figure 6.** Configurations SFBD, BFBD. Circadian optical efficiency profiles for summer/winter solstice (June 21, December 21) and equinox (March 21).

The circadian curves highlight that the BFBD configuration has – in comparison to SFBD – significantly flatter optical efficiency profiles over the day. A peak at solar noon is only visible for the winter solstice and is less pronounced. This can counteract the circadian variation of DNI and hence improves receiver operation by avoiding peak curtailment of thermal power.

As the adapted BFBD configuration is a mixture of SFBD and BFBD, its circadian behavior is between the two.

### 4.4 Different latitudes

In addition to the reference site in Yumen, China, the systems have been evaluated for

- Seville, Spain (37.4N, 5.9E)
- Ouarzazate, Morocco (31.0N, 6.9E)
- Antofagasta, Chile (24.1S, 69.1W, polar heliostat field is in the south)

Apart from the 180°-rotation for Antofagasta, the system designs are identical for all three sites. With equal tower heights and equal, pre-defined heliostat field outlines, potential differences in the optimum design are expected to be small. Thus, a comparison between the sites is reasonable, even without a re-design. Results for the annual optical efficiency – both absolute and normalized with the maximum value – for all sites/latitudes and all configurations are shown in Figure 7.

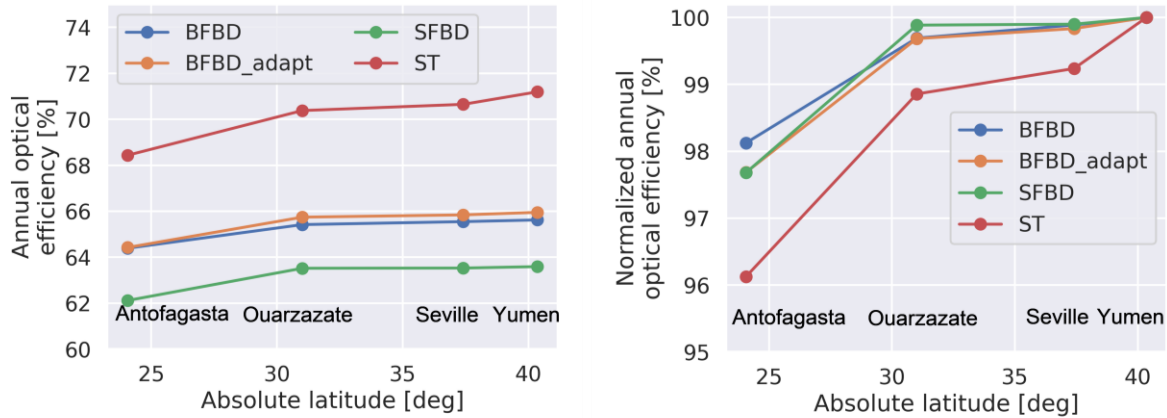


**Figure 7.** Annual optical efficiency for four sites/latitudes and four configurations. Left: absolute values. Right: values normalized with each system's maximum (Yumen).

All four configurations have their respective maximum in optical efficiency for the Yumen site, emphasizing that polar systems perform best at high latitudes. The normalization with the respective maximum value for each system reveals that the ST configuration suffers a more severe performance drop at lower latitudes compared to the Beam-Down counterparts. The latter are less sensitive with respect to latitude, with a relative decrease of less than 2% for the BFBD configuration, moving from Yumen to Antofagasta.

## 5. Conclusion

In small, modular CSP systems, use of polar heliostat fields reduces cosine losses. The integration of a beam-down reflector offers techno-economic advantages regarding thermo-hydraulic pumping losses and tower costs and furthermore enables innovative receiver concepts.

In this study, we suggest a bi-focus beam-down system, where the heliostats switch between two aim points depending on the sun position and hence significantly reduce the average incidence angle on the heliostat aperture.

Ray tracing assessment of annual, DNI-weighted optical efficiency proves that the BFBD configuration significantly reduces cosine losses, leading to higher annual, DNI-weighted optical efficiency. While a detailed investigation on the optical and thermo-hydraulic operation of a BFBD system is beyond the scope of this study, its flatter circadian profiles of optical efficiency could reduce peak dumping losses.

Further optimization potential is revealed by creating an enhanced design that combines the best aspects of both SFBD and BFBD. Bi-focus configurations are only techno-economically reasonable as part of a multi-unit system, where receivers shared by neighboring units reach a high utilization rate.

## Outlook

The suggested bi-focus beam-down concept already boosts the optical performance in a promising way, yet it also entails potential for further optimization. Future work should foremost include an algorithmic heliostat field design for multi-target systems. With this step being automated, an extensive parameter optimization for the overall system needs to be carried out. Regarding the beam-down reflectors, convex multi-faceted designs might further reduce spillage losses and secondary mirror area.



Overall, the suggested bi-focus beam-down system is an interesting option for modular, multi-unit CSP systems. This innovation could reduce Levelized Cost of Electricity significantly, by both increasing yield and curtailing costs. An application for high-temperature solar process heat is likewise conceivable.

## Data availability statement

The study is presented as-is, no additional underlying data is provided.

## Underlying and related material

The study is presented as-is, no additional related material is provided.

## Author contributions

Following the CRediT scheme (<https://credit.niso.org/>), Peter Schöttl contributed to the roles conceptualization, data curation, formal analysis, investigation, methodology, resources, software, visualization and writing (original draft). Gregor Bern and Francisco Torres contributed to conceptualization and to writing (review and editing).

## Competing interests

The authors declare that they have no competing interests.

## Funding

The project SOLBEADO, under which the work presented in this paper has been conducted, is funded by the German Federal Ministry for Economic Affairs and Climate Action (BMWK) under grant 03EE5083A. The authors of this publication are responsible for its contents.

## References

1. Dersch, J.; Binder, M.; Frantz, C.; Giuliano, S.; Gross, F.; Hasselbach, H. et al. (2022): CSP-reference power plant "Made in Germany". SOLARPACES 2020. AIP Publishing (AIP Conference Proceedings), p. 50003. DOI: 10.1063/5.0085877.
2. Vant-Hull, L. (2014): Issues with Beam-down Concepts. *Energy Procedia* 49, pp. 257–264. DOI: 10.1016/j.egypro.2014.03.028.
3. Bellos, E. (2023): Progress in beam-down solar concentrating systems. In *Prog Energy Combust* 97, p. 101085. DOI: 10.1016/j.pecs.2023.101085.
4. Buck, R.; Schwarzbözl, P. (2018): 4.17 Solar Tower Systems. *Comprehensive Energy Systems*. Elsevier, pp. 692–732. DOI: 10.1016/B978-0-12-809597-3.00428-4.
5. Arbes, F.; Landman, W.; Weinrebe, G.; Wöhrbach, M.; Gebreiter, D.; Estebaranz, J. et al. (2019): Multi tower systems and simulation tools. SOLARPACES 2018. AIP Publishing (AIP Conference Proceedings), p. 30004. DOI: 10.1063/1.5117516.
6. Siala, F.; Elayeb, M. (2001): Mathematical formulation of a graphical method for a non-blocking heliostat field layout. *Renewable Energy* 23 (1), pp. 77–92. DOI: 10.1016/S0960-1481(00)00159-2.
7. Leonardi, E.; Pisani, L.; Les, I.; Mutuberria, A.; Rohani, S.; Schöttl, P. (2019): Techno-Economic Heliostat Field Optimization: Comparative Analysis of Different Layouts. *Solar Energy* 180, pp. 601–607. DOI: 10.1016/j.solener.2019.01.053.

8. Schöttl, P.; Bern, G.; Nitz, P.; Torres, F.; Graf, L. (2022): Raytrace3D by Fraunhofer ISE. Accurate and Efficient Ray Tracing for Concentrator Optics. Available online at <https://www.ise.fraunhofer.de/content/dam/ise/de/downloads/pdf/raytrace3d.pdf> .
9. Schöttl, P.; Ordóñez Moreno, K.; van Rooyen, D.; Bern, G.; Nitz, P. (2016): Novel sky discretization method for optical annual assessment of solar tower plants. *Solar Energy* 138, pp. 36–46. DOI: 10.1016/j.solener.2016.08.049.
10. METEOTEST (2015): *Meteonorm Handbook Part I. Software (Version 7.1 / July 2015)*. Available online at [http://meteonorm.com/images/uploads/downloads/mn71\\_software.pdf](http://meteonorm.com/images/uploads/downloads/mn71_software.pdf) .
11. Noone, C.; Torrilhon, M.; Mitsos, A. (2012): Heliostat field optimization. A new computationally efficient model and biomimetic layout. In *Solar Energy* 86 (2), pp. 792–803. DOI: 10.1016/j.solener.2011.12.007.